Investigations of 600-V GaN HEMT and GaN Diode for Power Converter Applications

Radoslava Mitova, Rajesh Ghosh, Uday Mhaskar, Damir Klikic, Miao-Xin Wang, and Alain Dentella

***Abstract*—Power switching devices based on wide bandgap semiconductor materials, such as silicon carbide (SiC) and gallium nitride (GaN) offer superior performance such as low switching and conduction losses, high voltage, high frequency, and high temperature operation. In this paper, a 600-V GaN switch and a 600-V GaN diode were tested in detail to understand the GaN device capabilities with respect to equivalent silicon-based devices such as IGBT and MOSFET. Detailed experimental loss models are developed and compared with datasheet models. Experimental setup of different power converters such as boost, buck–boost, and half-bridge inverter and associated comparative experimental results are presented. This paper also presents the investigations into the effectiveness of using GaN devices and higher switching frequencies in reducing the total size and cost of power conversion equipment such as an online UPS system.**

***Index Terms*—Boost converter, gallium nitride high electron mobility transistor (GaN HEMT), inverter, power factor corrected (PFC), wide bandgap (WBG) technology.**

I. Introduction

THERE is an ever increasing market pressure to reduce the size of all power electronic products for the same output power and reliability. Furthermore, a lot of energy standards are in place demanding high energy efficiency of a product [1]. In order to address these needs, the industry is looking for advanced power switching devices [2], [3]. The newer devices must switch at much higher speed (20–40 times), exhibit low switching and conduction losses and operate at much higher temperature (>200 °C) than the traditional silicon (Si)-based devices such as IGBT and MOSFET [2]–[5].

Wide bandgap (WBG) materials such as silicon carbide (SiC), gallium nitride (GaN) and Diamond [2]–[5] have been discovered to have nearly matching physical, electrical, and thermal characteristics for the device of interest [2]–[5]. Research and development is already in place to develop power switching devices based on these materials and to continuously improve their characteristics [3]–[13]. Their fast switching speed and low switching and conduction losses help increase the power density and efficiency of power conversion equipments, while their high-temperature operating capability makes them very attractive for harsh environmental applications [3]–[13]. It is reported that such characteristics are not achievable in Si-based devices as the Si technology has reached at the verge of its maturity [11]–[13], [19]. Compared to GaN, the SiC device technology is in an advanced stage, where particularly, SiC-based diodes have proven their maturity and robustness in industry applications [14]–[17]. However, due to its higher cost (10–15 times higher than equivalent Si devices), its use has been limited mostly for critical applications. On the other hand, the predicted GaN device price in the near future is expected to be in the range of today's equivalent Si device [18]. Due to its attractive pricing, GaN devices are expected to be much more acceptable to the industry in the near future than SiC devices.

Unlike SiC devices, GaN devices are not widely available in the market. Some GaN manufactures like efficient power conversion provide GaN devices up to 200-V rating, and can be used only in low voltage (LV) applications. A number of applications, however, demand devices with voltage rating of 600 V and above. As of now, only few device manufacturers are able to provide 600-V GaN switches and diodes. Many other manufacturers such as *IR*, *GaNSystems*, *MicroGaN,* and *Transphorm* are developing high-voltage and high-current GaN devices, which are expected to be available as samples from early 2014.

This paper focuses on the advantages of using forthcoming GaN power devices [20] in place of Si-based devices (IGBT, MOSFET) in various power electronic converters such as boost [21]–[24], buck–boost [25], [26], inverter [27], [28], and finally, in a single-phase online UPS system [29], [30]. Different experimental prototypes have been built using one set of 600-V GaN high electron mobility transistor (HEMT), and 600-V GaN diode to validate the theoretical predictions. The aforementioned devices were obtained from *Transphorm* as samples. These devices are soon expected to be commercially available. All the results presented in this paper are based on a single set of GaN HEMT and diode from *Transphorm*. This paper is organized as follows:

Section II briefly describes GaN switch and diode parts. In Section III, we experimentally characterize their switching, conduction loss, and short-circuit behavior. Section IV discusses the applications of the devices to different power converters such as boost converter and half-bridge inverter. The effect of paralleling GaN switches and diodes is also addressed. In Section V, we provide a comparison of performance between GaN switch, IGBT, MOSFET, GaN diode, and Si and SiC diodes. In Section VI,

Manuscript received March 4, 2013; revised June 25, 2013 and September 4, 2013; accepted October 7, 2013. Date of current version January 10, 2014. Recommended for publication by Associate Editor I. Omura.

R. Mitova, M.-X. Wang, and A. Dentella are with the Schneider Electric, Strategy and Innovation, 38050 Grenoble, France (e-mail: radoslava.mitova@schneider-electric.com; miao-xin.wang@schneider-electric.com; alain_dentella@mail.schneider-fr).

R. Ghosh and U. Mhaskar is with the Schneider Electric, Bangalore 560066, India (e-mail: rajesiisc@yahoo.co.in; udaymhaskar@gmail.com).

D. Klikic is with the Schneider Electric, N. Billerica, MA 01862 USA (e-mail: damir.klikic@schneider-electric.com).

Color versions of one or more of the figures in this paper are available online at http://ieeexplore.ieee.org.

Digital Object Identifier 10.1109/TPEL.2013.2286639

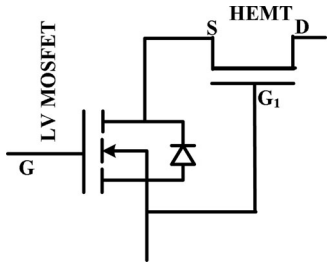

Fig. 1. Cascade GaN device structure.

we provide an analysis of the benefits of using GaN with respect to IGBT in a 1.5-kW online UPS system. Section VII discusses the issues, concerns and lessons learnt. Finally, the conclusion is drawn in Section VIII.

II. GaN Power Switch and GaN Diode

This section briefly discusses the GaN HEMT and GaN diode used in this paper.

A. GaN Switch and GaN Diode

The basic GaN HEMT structure is normally ON type [31]. In order to increase its acceptability and applicability, manufactures use the cascade configuration to convert it into a normally OFF type device [31]. It consists of a LV-rated Si MOSFET (typically 30 V and low on-state resistance) connected in series with the GaN HEMT as shown in Fig. 1. The resultant device (hereafter, termed as the GaN switch) is turned ON and OFF by applying a voltage pulse on the LV MOSFET gate. The HEMT channel can conduct current in both directions when it is gated ON.

As shown in Fig. 1, the GaN HEMT does not have any internal body diode. The on-state current, irrespective of its direction, flows through the channels of both, the MOSFET and GaN HEMT, when the GaN switch is turned ON. Due to low on-state resistance of the LV MOSFET, the conduction loss mainly takes place in the GaN HEMT. In most converter applications such as the boost [21]–[24], buck, and buck–boost [25], [26], the MOSFET body diode does not conduct. In case of a half-bridge inverter, operated with complementary gating pulses [28], the MOSFET body diode may conduct during the dead time when both switches are OFF. During this time, the MOSFET body diode may incur high conduction loss. Soon after the dead time, the incoming GaN switch is gated ON and the current gets shifted from the body diode to its parent MOSFET channel, resulting in low conduction loss. Due to low dead time ($<$100 ns), the conduction loss in the MOSFET body diode is negligible. Further, the MOSFET turns ON, and its body diode recovers at near zero voltage, resulting in negligible switching and recovery losses during this current transfer [32]. As per the manufacturer, the GaN diode used in this paper is a high voltage Schottky diode [33].

B. Gate Resistor

The GaN switch is turned ON and OFF by controlling the internal MOSFET. The gate resistor actually controls the turn ON and OFF switching times of the MOSFET. The MOSFET incurs low switching losses as it switches at low voltage. Hence, unlike the Si-based devices, the gate resistor plays a negligible role on the switching performance of the GaN switch. Further, the GaN device manufacturers recommend driving the GaN switch directly by the gate driver output without connecting any gate resistor. A gate resistor of 10–20 Ω helps reduce the gate voltage oscillations around the switching period as shown in Fig. 2(a) and (b), respectively.

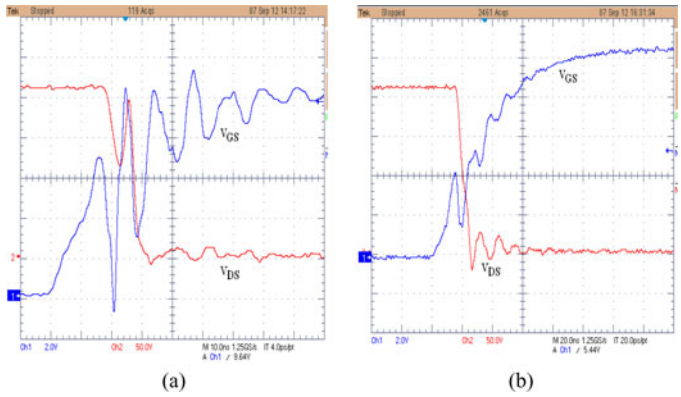

Fig. 2. Gate to source waveform at full load with (a) zero ohm and (b) 10 Ω gate resistors.

TABLE I
Ratings of GaN Switch and Diode

Parameters	GaN Switch		GaN diode
Voltage rating	600V		600V
Gate voltage	±18V		-
Gate threshold voltage	1.8V		-
Current rating	20A @25°C 12.5A @ 100°C		9.2A @100°C 6.2A @ 125°C
On state resistance/ on state voltage drop	0.15Ω @ 25°C		1.3V @ 6A, 25°C
$T_{j(max)}$	150° C		150° C
$R_{\theta\text{-}JC}$	1.0°C/W		1.8°C/W
Input capacitance	815PF	@ V_{GS}=0 V, V_{DS}=100V, f =1MHz	-
Output capacitance	95PF		-
Reverese transfer capacitance	2.5PF		-
Turn-on delay	4.4ns	@ V_{DS} =480 V, V_{GS}= 0-10 V, I_D = 11 A, R_G= 2 Ω	-
Turn-off delay	13ns		-
Rise time	2ns		-
fall time	3.5ns		-

C. GaN HEMT and GaN Diode Ratings

The important datasheet specifications of the GaN switch and the GaN diode used in this paper are tabulated in Table I. The GaN switch and diode are packed in TO-220 package.

III. GaN Switch and Diode Characterization

Device characterization is essential to predict its switching and conduction loss. This is required to design the thermal

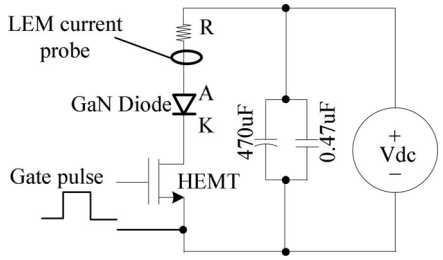

Fig. 3. GaN switch and diode conduction characterization setup.

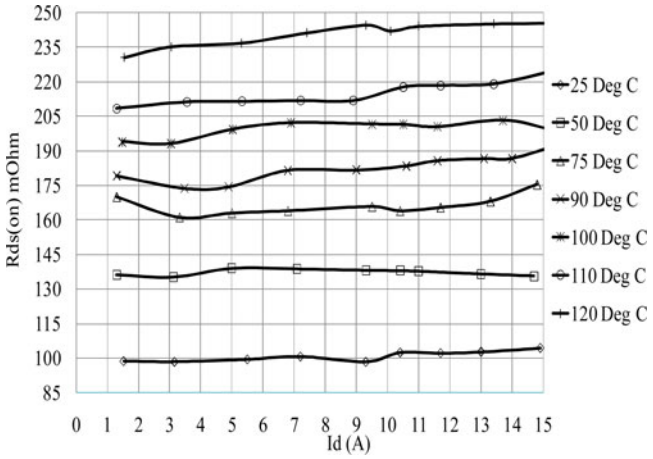

Fig. 4. GaN switch measured $R_{\mathrm{ds(on)}}$ characteristics.

system of a power converter and to estimate the converter efficiency. Normally, the device manufacturer presents different loss curves under various operating conditions [32]. These curves could be theoretical or experimental. It is, therefore, necessary to verify the device characteristics experimentally before using them. In this section, the experimental loss models of the GaN switch and GaN diode have been established, which are compared against the predicted loss models, developed using the datasheet.

A. GaN Switch on-State Resistance Characterization

Fig. 3 shows the simplified schematic of the on-state device characterization setup for the GaN switch. A short duration current pulse was forced through the switch by turning it ON by a short gate pulse. The conduction voltage drop $(V_{\mathrm{ds(on)}})$ across the drain to source terminals, and the drain current I_d were captured on an oscilloscope. The experiment was repeated at different junction temperatures, where the GaN switch was heated up to the desired temperature using a heating resistor before testing. The on-state resistance $R_{\mathrm{ds(on)}}$ at operating temperature t_j and drain current I_d can be given by (1)

$$R_{\mathrm{ds(on)}}\big|_{I_d,t_j} = \frac{V_{\mathrm{ds(on)}}}{I_d}. \tag{1}$$

The measured $R_{\mathrm{ds(on)}}$ characteristics with respect to drain current and temperature are shown in Fig. 4. It strongly depends on the junction temperature and does not depend on the drain current. For modeling purpose, all the data points corresponding

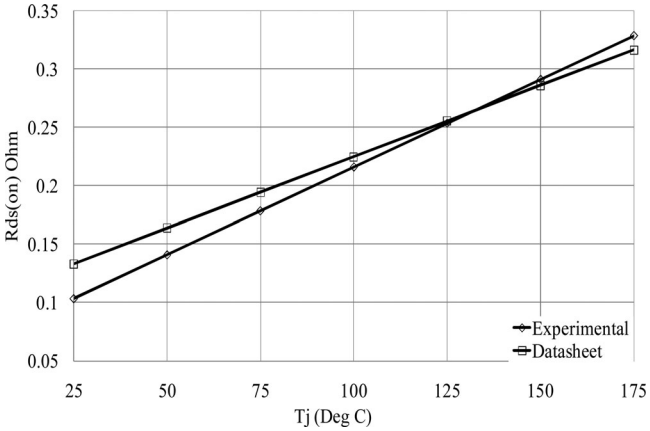

Fig. 5. Comparison of GaN switch $R_{\mathrm{ds(on)}}$ characteristics.

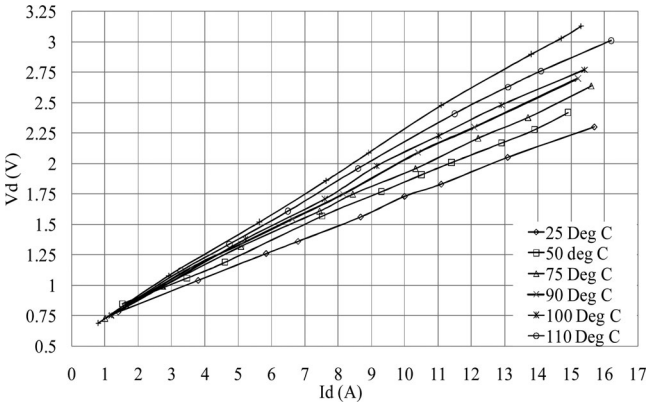

Fig. 6. GaN diode measured $V_{d(\mathrm{on})}$ characteristics.

to a particular temperature have been lumped into a single value. The experimental $R_{\mathrm{ds(on)}}$ model obtained using curve fitting technique is given by (2). It matches well with the datasheet characteristics as shown in Fig. 5

$$R_{\mathrm{ds(on)}}|_{t_j} = 1.5T_j + 66\ \mathrm{m\Omega}. \tag{2}$$

B. GaN Diode on-State Voltage Drop Characterization

The experimental setup shown in Fig. 3 was also used to characterize the conduction loss of the GaN diode. Using the method described in the Section III-B, the diode forward voltage drop at different case temperatures t_j and current I_d was obtained as shown in Fig. 6. The conduction drop depends both on the temperature and the current. Using curve fitting, the conduction voltage drop model was obtained as follows:

$$V_d|_{T_j,I_d} = \left[5.9 \times 10^{-2} + 9.0 \times 10^{-4} T_j\right] I_d + 0.6\ \mathrm{V}. \tag{3}$$

The aforememtioned model matches well with the datasheet as shown in Fig. 7. The positive temperature coefficient allows us to parallel multiple GaN diodes for higher power application.

C. GaN Switch Switching Loss Characterization

The test setup used for switching characterization, known as double pulse test (DPT) [6], [7], [9], is shown in Fig. 8. The

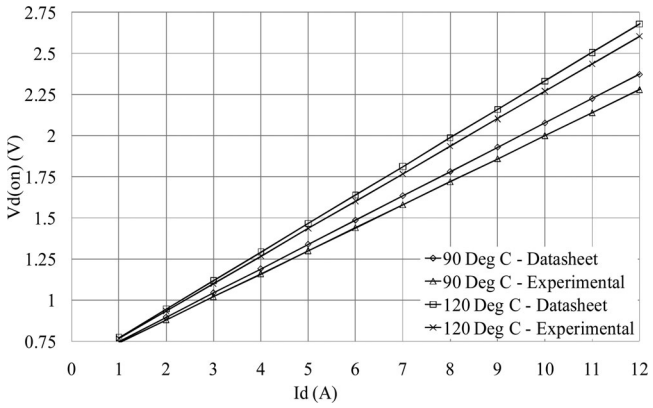

Fig. 7. Comparison of GaN diode $V_{d(\mathrm{on})}$ characteristics.

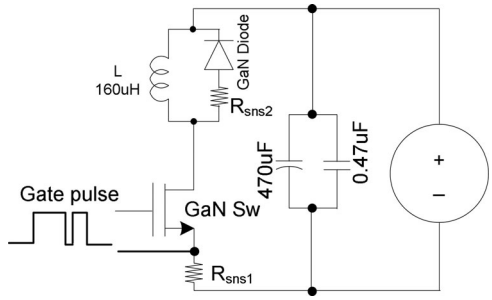

Fig. 8. Double pulse test setup for switching loss characterization.

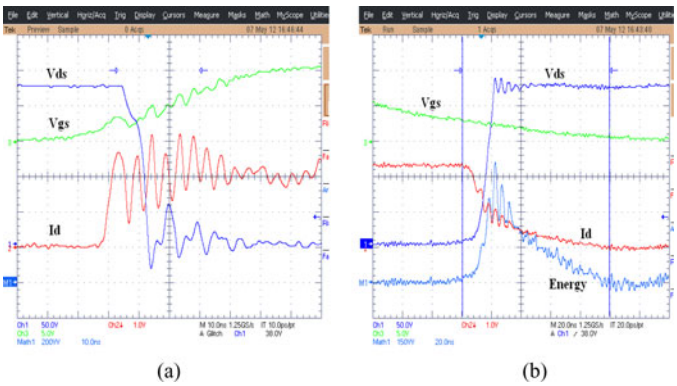

Fig. 9. GaN switching waveforms: (a) turn-on and (b) turn-off.

GaN switch was gated ON using a double pulse gate voltage. The device current was measured by measuring the voltage drop across the current sense resistor R_{sns1}. The drain to source voltage, drain current and switching time around the switching instant were captured in an oscilloscope to calculate the switching energy. Sample waveforms are shown in Fig. 9(a) and (b). The experiment was conducted at 240 V dc and at different currents. The theoretical and experimental turn-on and turn-off switching energy models are given by (4a) and (4b), and (5a) and (5b), respectively

$$E_{\mathrm{on}(T)} = \left[20.10 \times 10^{-1} I_d\right] \frac{V_{\mathrm{dc}}}{240}\ \mu\mathrm{J} \tag{4a}$$

$$E_{\mathrm{off}(T)} = \left[137.40 \times 10^{-1} I_d\right] \frac{V_{\mathrm{dc}}}{240}\ \mu\mathrm{J} \tag{4b}$$

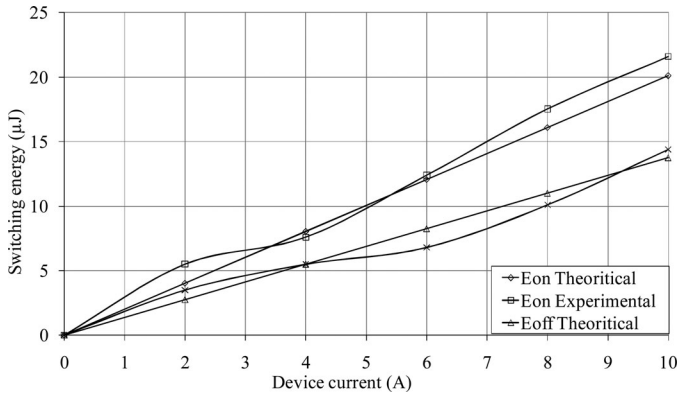

Fig. 10. Comparison of GaN switch switching characteristics.

$$E_{\mathrm{on}(E)} = [5.30 \times 10^{-3} I_d^3 - 5.75 \times 10^{-2} I_d^2 + 21.9 \times 10^{-1} I_d + 1.00 \times 10^{-2}] \frac{V_{\mathrm{dc}}}{240}\ \mu\mathrm{J} \tag{5a}$$

$$E_{\mathrm{off}(E)} = [2.40 \times 10^{-2} I_d^3 - 31.60 \times 10^{-2} I_d^2 + 22.23 \times 10^{-1} I_d + 4.30 \times 10^{-2}] \frac{V_{\mathrm{dc}}}{240}\ \mu\mathrm{J}. \tag{5b}$$

The switching characteristic obtained using this model is compared against theoretical characteristic in Fig. 10. Although, the experimental switching characteristics nearly match the theoretical one; there is, however, some difference between them. This difference may be attributed to the error that gets introduced in the computation of switching energy from the oscillatory drain current and voltage waveforms as seen from Fig. 9. It was also observed that at lower current, the device junction capacitor takes a longer time to charge or discharge. This results in longer switching durations, and hence, higher switching losses as compared to datasheet values.

D. GaN Diode Reverse Recovery Characterization

A similar experimental setup (see Fig. 8) was used to obtain the reverse recovery characteristics of the GaN diode. The diode current, voltage drop, and the time around the switching instant was captured using an oscilloscope. The experiment was carried out at a forward current of 5 A and 300 V dc for two different temperatures, 25 °C and 125 °C, respectively. The respective energies were computed to be 2.98 μJ and 3.05 μJ. It shows that the reverse recovery energy does not depend much on the operating temperature. The average reverse recovery charge is 10 nC. The reverse recovery charge model is given by (6) [34], where the constant K_{Qr} is given by (7)

$$Q_{rr} = K_{Qr} . \sqrt{I_F} \tag{6}$$

$$K_{Qr} = \left. \frac{Q_{rr}}{\sqrt{I_F}} \right|_{I_F = 5A}. \tag{7}$$

Since no data were available in the diode datasheet for the reverse recovery charge, we could not compare the results with datasheet parameters.

E. GaN Switch Overcurrent Characterization

A converter is subjected to different types of short-circuit failure [38], where the devices carry large current for a short duration before the gate driver detects it and stops the gating pulses [35]. The fault detection and clearance time is typically <6 μs. The modern IGBT's can withstand worst case short circuit for 10 μs duration [35]. In case of GaN switch under consideration, complete datasheet was unavailable. The short-circuit capability was tested experimentally.

A 600-V rated device is normally used in applications having a nominal dc bus voltage less than or equals 400 V. Hence, in order to qualify for the short-circuit capability, the device must withstand worst case short circuit for 10 μs duration with 400 V across it. In order to test this capability, the GaN switch was soldered directly on the terminals of a 470 μF, 450 V electrolytic capacitor. The capacitor was charged to different voltages (gradually increasing from 10 V) before it was shorted through the GaN switch by gating "on" the switch only once for 10 μs duration by 12 V gate voltage. At each voltage level, the sample was tested for 10 times to ensure consistency. The device voltage, current, and short-circuit time were captured on an oscilloscope. It was seen that for 12-V gate drive voltage, the maximum drain current was limited to around 70 A for any drain to source voltage beyond 30 V. A sample waveform at a dc voltage of 150 V is shown in Fig. 11(a), where the current was measured using Rogowski coil (20 A/V). The first sample was failed at around 220 V, while the others failed between 220 and 280 V. Fig. 11(b) shows the measured power and energy that the device was able to handle up to 200 V dc for 10 μs duration without any failure.

The failure of the GaN switch at a dc voltage less than 400 V indicates that unlike the IGBT [35], the GaN switch under consideration does not have required short-circuit capability. However, it can safely tolerate worst case short circuit for 10 μs duration up to a dc voltage of 200 V.

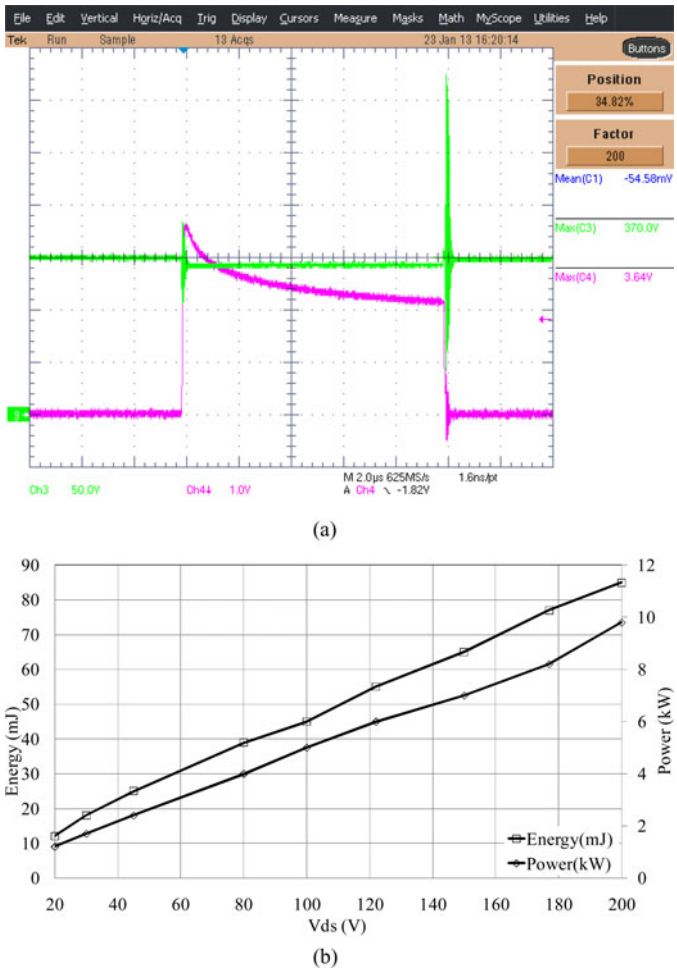

Fig. 11. (a). Short-circuit waveform of GaN HEMT for 10 μs: [$V_{\rm DS}$ (green trace 50 V/div), I_D (pink trace 20 A/div)]. (b) Short-circuit characteristics of GaN HEMT for 10 μs.

IV. Application of GaN Switch and Diode

In this section, we discuss the applications of GaN switch and the GaN diode for different power converter configurations such as half-bridge inverter [28], boost converter [21], and buck–boost converter [25], which are widely used in single-phase online UPS systems [29].

A. DC–DC Boost Converter

A 500-W dc–dc boost converter [21] prototype was built with single GaN switch and GaN diode. The schematic of the boost converter is shown in Fig. 12. The input and output voltages were 120 and 210 V, respectively. The switching frequency and the output power were varied from 50 to 500 kHz, and 100 to 500 W, respectively. Different valued inductors were used for different switching frequency ranges. Between 50 and 150 kHz, a 450 μH inductor was used, while 300 μH and 150 μH inductors were used for the switching frequency ranges 150–300 kHz and 300–500 kHz, respectively. All the inductors were fabricated on EE type ferrite cores of N87 low loss material. The effect of using

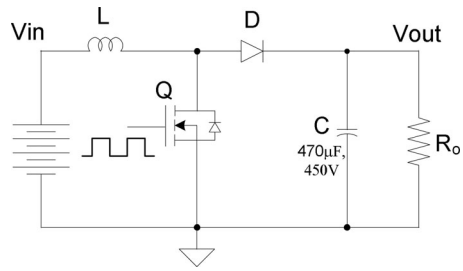

Fig. 12. Boost converter schematic.

different inductors on the efficiency was ensured to be negligible. Fig. 13(a) shows the measured efficiencies under different operating conditions. The maximum efficiency was obtained at around 100-kHz switching frequency. Beyond 100 kHz, the converter efficiency decreases due to increased switching loss, inductor core loss and high-frequency copper loss. Also, during this time, the maximum efficiency point gets shifted to higher loads. The switching loss contributes a significant portion of the total losses at light load. Fig. 10 also indicates this fact that the measured switching energy is more at less current compared to its theoretical values. At higher load, however, the switching

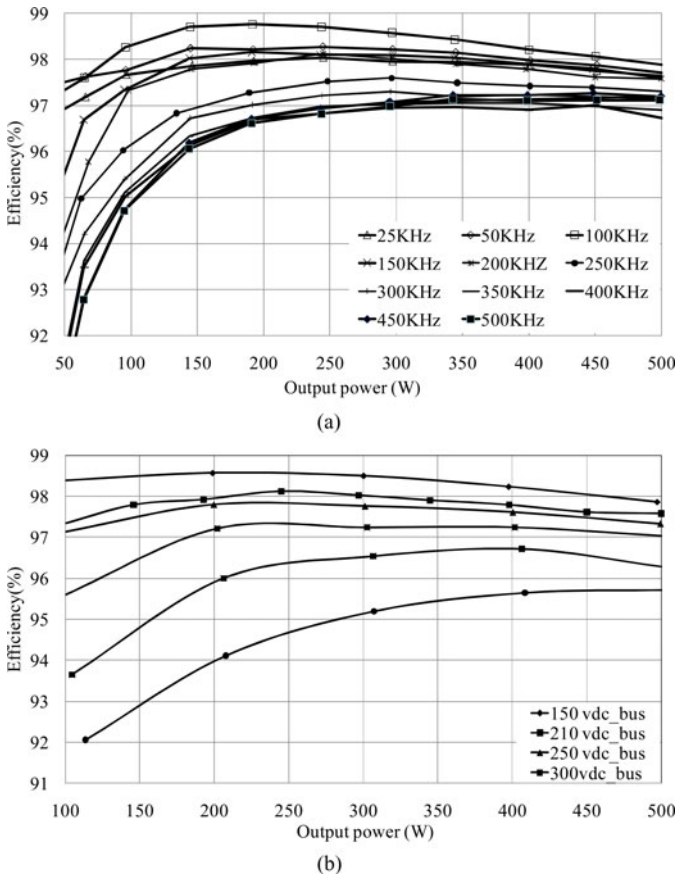

Fig. 13. Boost converter measured efficiencies: (a) at different switching frequencies and (b) at different output voltages.

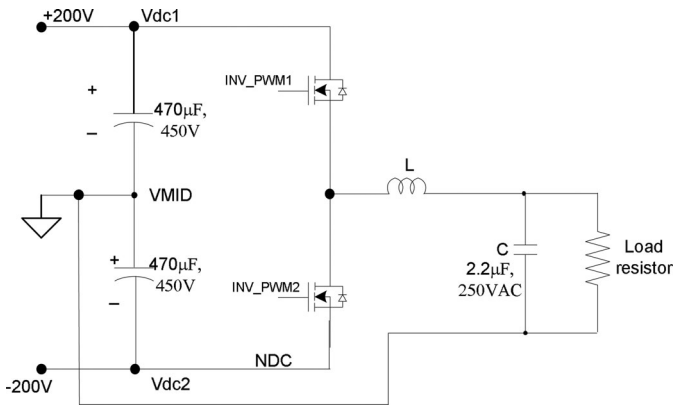

Fig. 14. Circuit schematic of half-bridge inverter.

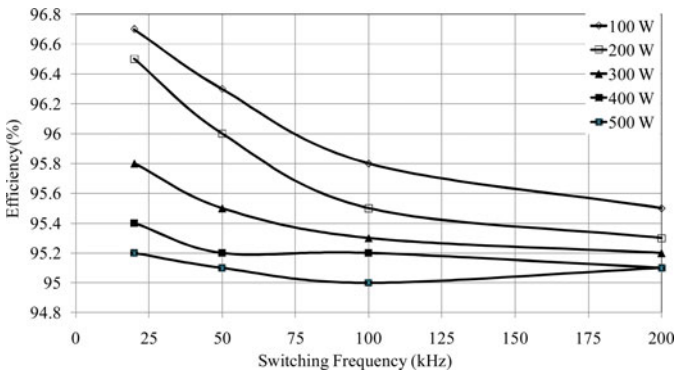

Fig. 15. Half-bridge inverter measured efficiencies.

loss occupies a small percentage of the total losses. Fig. 13(b) shows the dependence of the converter efficiency on the output voltage (i.e., on the duty cycle), where the input voltage and switching frequency are 120 V and 200 kHz, respectively. It was seen that the efficiency curves follow similar trend as with 210-V dc bus. As the switching loss increases at higher dc bus voltage, the converter efficiency decreases.

B. Single-Phase Half-Bridge Inverter

A 1-kW half-bridge inverter [28] prototype was built using two GaN switches, operated in a complementary fashion. The circuit schematic of the inverter is shown in Fig. 14. A split dc bus of ± 200 V is used to generate a 120-V, 50-Hz output. The dead time between the top and bottom switches was set at 100 ns, which was set based on the value of the gate resistor (10 Ω), the effective gate to source capacitor (1000 pF) and the minimum gate to source threshold voltage (1.35 V). Finally, the dead time was measured between the instants of one gate to source voltage going above, and other going below 1.35-V level. Similar to the boost converter, the inverter was operated at different switching frequencies with different valued inductors. Four inductors; 5, 2, 1, and 0.5 mH, were used for 20, 50, 100, and 200 kHz switching frequencies, respectively. The experimental results are plotted in Fig. 15. Similar to the boost converter results, it can be seen that the switching frequency, and hence, the switching loss has higher impact on efficiency at light load and relatively low impact at higher loads. In other words, due to very low switching loss of the GaN switch, the conduction loss is dominant factor at higher loads, where switching losses present only very small percentage of the total losses regardless of the switching frequency.

C. Paralleling the GaN Switch and Diode

The resistive forward characteristics of the GaN switch and GaN diode are favorable for parallel operation. In order to test this capability, the dc–dc boost converter [21] presented in Section IV-A is modified for two paralleled GaN switches and two paralleled GaN diodes. The GaN switch Q shown in Fig. 12 was realized by two GaN switches connected in parallel. Similarly, two GaN diodes were connected in parallel to realize the diode D in Fig. 12. Fig. 16 shows the measured comparative efficiency results for two different output voltages.

It was observed that at 400-V output voltage, parallel device always offers higher efficiency than a single device due to reduction in conduction loss. In the case of 210-V output, single device offers little higher efficiency up to 300 W output power, beyond which the parallel device offers higher efficiency. At 210-V output, the GaN switch operates with low duty cycle as compared to the case with 400-V output. Similar to the results presented in Fig. 13, the switching loss contributes a significant portion of the total losses at light load. As a result, single device

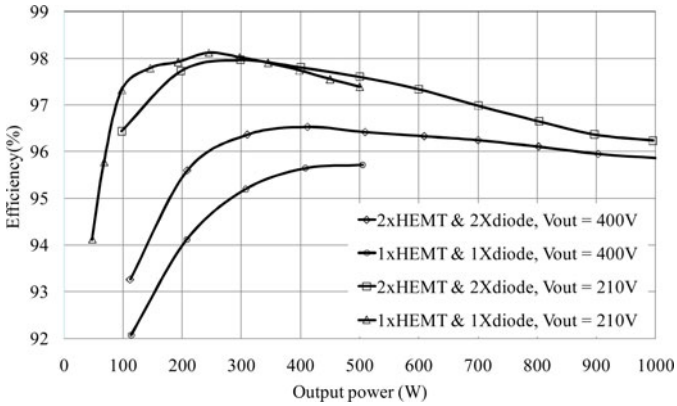

Fig. 16. Boost converter efficiency with single and parallel devices.

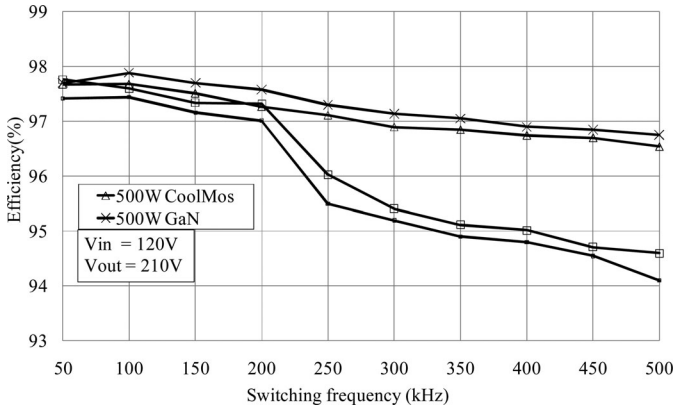

Fig. 17. Boost converter efficiency: GaN Versus CoolMOS.

offers higher efficiency at light load. A similar characteristic is presented in [36]. However, this trend was not seen in 400 V output case, as due to higher duty cycle, the conduction loss dominates over the switching losses at light load.

V. Comparison of GaN With Si and SiC

In this section, the performance of the GaN switch is compared against the equivalent Si-based devices such as IGBT and MOSFET, and the GaN diode is compared with equivalent Si and SiC diodes. This evaluation helps us understand where the GaN technology stands with respect to today's Si and SiC technology.

A. GaN Switch Versus MOSFET

In this evaluation, all the devices were tested on a converter under the same operating conditions. The performance was compared in terms of the measured efficiencies. In comparison with MOSFET, an equivalent CoolMOS part IPP60R199CP by Infineon [35] was considered. The device was tested on the boost converter platform discussed in Section IV-A. Only the GaN switch was replaced with the CoolMOS, while the GaN diode still served as the boost diode. Fig. 17 shows the measured comparative efficiencies with GaN and CoolMOS devices. The performance of the GaN switch is slightly better than, and very close to the CoolMOS device upto 400-kHz switching frequency.

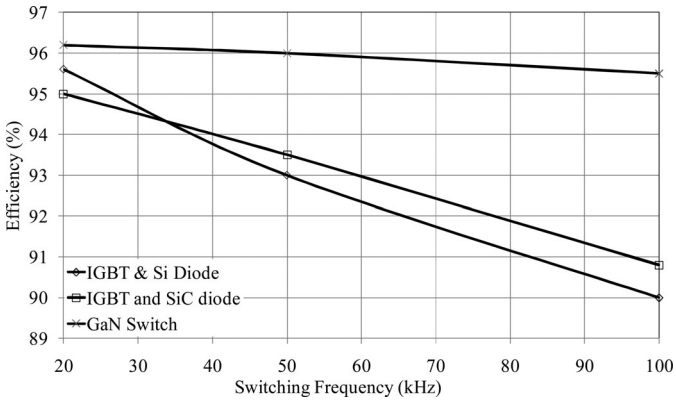

Fig. 18. Half-bridge inverter comparative efficiencies with GaN switch, IGBT with Si body diode, and IGBT with SiC body diode.

TABLE II
Diodes Recovery Losses

Diode	Test conditions	Losses
Si FFPF10UP60S 600V, 10A, trr 58ns	25°C, 5A, 300V 125°C, 5A, 300V di/dt 450A/μs	45μJ 90μJ
SiC IDH10SG60C 600V, 10A trr 10ns	25°C, 5A, 300V 125°C, 5A, 300V di/dt 450A/μs	2.6μJ 3.14μJ
GaN 600V, 6A,trr 30ns	25°C, 5A, 300V 125°C, 5A, 300V di/dt 450A/μs	2.98μJ 3.05μJ

Beyond 400 kHz, the switching losses in CoolMOS start increasing rapidly as compared to GaN. As a result, a reduction in efficiency was observed in CoolMOS beyond 400 kHz as compared to GaN.

B. GaN Switch Versus IGBT

The GaN switch performance was compared with the IGBT on the half-bridge inverter prototype described in Section IV-B. The circuit configuration is as shown in Fig. 14. Two different IGBT's were considered. These are 1) 600-V, 13-A IGBT (IRGB20B60PD1) with Si body diode by IR and 2) 600-V, 48-A IGBT (IXGH48N60C3C1) by IXYS, with silicon carbide (SiC) body diode. The inverter was tested at different switching frequencies with a 200-W resistive load. The comparative experimental results are presented in Fig. 18. The efficiency, due to high switching loss, falls rapidly for IGBTs, and monotonically for GaN switch. Hence, the GaN offers superior performance over the given IGBTs.

C. GaN Diode Versus Si and SiC Diodes

This comparison is based on the measured reverse recovery characteristics obtained using the setup shown in Fig. 8. The comparative test results are tabulated in Table II and the reverse recovery current waveforms corresponding to 25 °C case temperature are shown in Fig. 19. It shows that the reverse recovery characteristic of the GaN diode is very similar to the SiC diode, and is much better than the equivalent Si diode. The increase

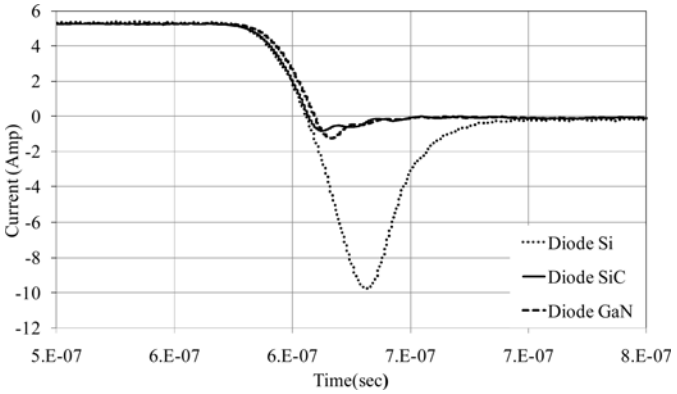

Fig. 19. Reverse recovery performances of GaN, Si, and SiC diodes.

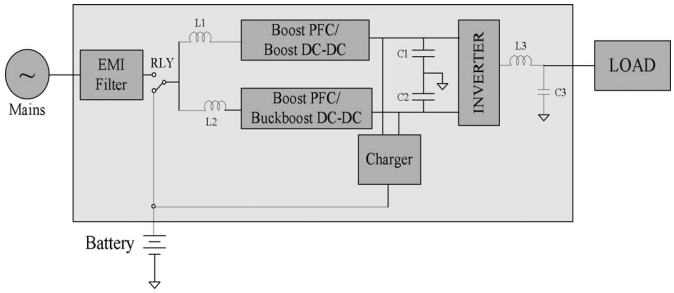

Fig. 20. Single line diagram of double conversion UPS.

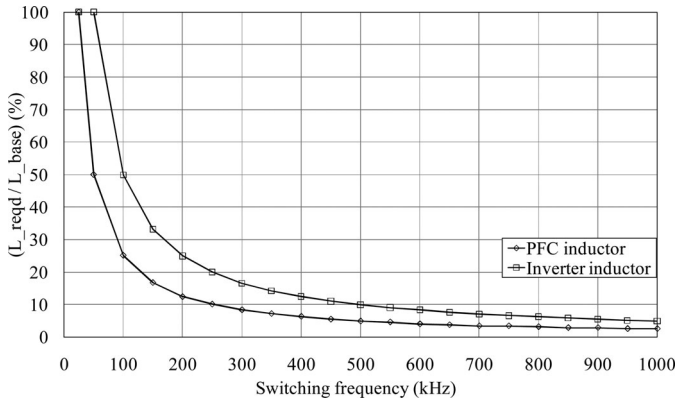

Fig. 21. Inductance variation with respect to switching frequency.

in reverse recovery loss from 25 to 125 °C for the GaN diode was less than that of the SiC diode. In other words, the reverse recovery loss in the GaN diode is less dependent on the operating junction temperature compared to SiC diode. Although, the recovery loss in SiC diode is less at 25 °C compared to GaN diode, it is, however, more at 125 °C case temperature. Therefore, the use of GaN diode will result in slightly less switching loss around rated operating condition compared the SiC diode.

VI. Benefit Analyses

The benefits of using GaN devices in power converters as compared to the Si-based devices are listed as follows:

1) the converter can operate at very high switching frequency to reduce the size of inductors and capacitors;
2) its low switching and conduction losses help reduce the thermal challenges such as, cooling and heat sink design;
3) due to (1) and (2), a compact and high power density converter is realizable at low cost;
4) higher converter efficiency helps meet different stringent energy standards.

This section also discusses the benefit assessment, with respect to cost, efficiency, and volume on a GaN-based 500-W online (double conversion) UPS system prototype. All analyses and results are compared with respect to an equivalent IGBT-based online UPS system (baseline).

The block diagram of the online UPS system, under investigation, is shown in Fig. 20. The UPS system is designed for 120-V, 50-Hz input and output. A 48-V battery serves as the dc input. In *online* mode, two power factor corrected (PFC) boost converters feed the split dc bus of ± 210 V from the mains; one feeds the positive dc bus, while other the negative dc bus from the positive and negative half line cycles, respectively. In *on-battery* operation, one boost converter [21] and one buck–boost converter [25] were used to feed the split dc buses from the battery. The desired output voltage was obtained from the split dc bus using a half-bridge inverter [28]. The power converter modules of the GaN UPS, and the baseline UPS were operated at 200 and 25 kHz, respectively.

A. Energy Storage Elements Size Reduction Benefit

Inductors and capacitors are the main energy storage elements in power converters. Three major inductors L_1, L_2, and L_3, and three major capacitors C_1, C_2, and C_3 were used. The electrolytic (EL) capacitors C_1 and C_2 form the dc buses. Their value/size cannot be reduced by increasing the switching frequency as it depends on many other factors such as, hold up time, dc bus voltage stability, and low-frequency ripple voltages, which are independent of switching frequency. Therefore, there was no saving from the EL capacitors. The inductors of the baseline UPS are made of powder iron cores (CoolMu). These cannot be used for high switching frequency application due to higher core losses. The inductors of GaN UPS were realized using ferrite EE cores (N87 material) having low core loss.

Fig. 21 shows the required inductance as a percentage of the baseline inductance for the PFC inductors (L_1 and L_2) and the inverter filter inductor L_3 with respect to switching frequency for the same peak-to-peak ripple current of 30% at full load. As seen from Fig. 21, the required inductance value falls sharply between 25 and 200 kHz. Beyond 200 kHz, the inductance values decreases monotonically. The inductor size and footprint also have similar trends.

In the baseline UPS, a 40-μF polypropylene capacitor C_3 has been used as the output filter capacitor, which corresponds to a cutoff frequency of 1/20 of the baseline switching frequency. With the same cutoff frequency, the required value of the filter capacitor for the GaN UPS is around 4.7 μF. The volume of the 4.7-μF capacitor was found around 40% of the volume of a 40-μF capacitor.

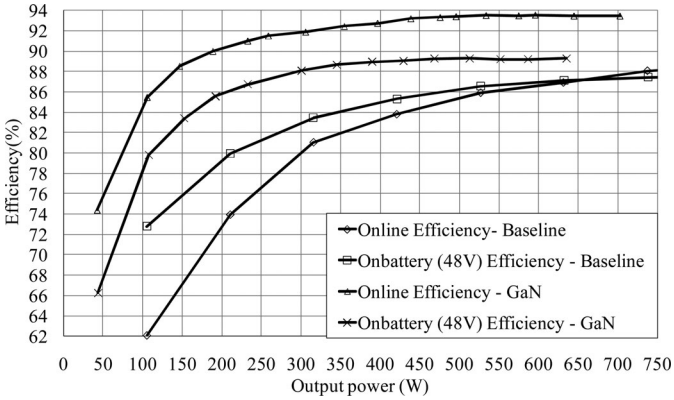

Fig. 22. Comparative efficiencies of GaN UPS and baseline UPS.

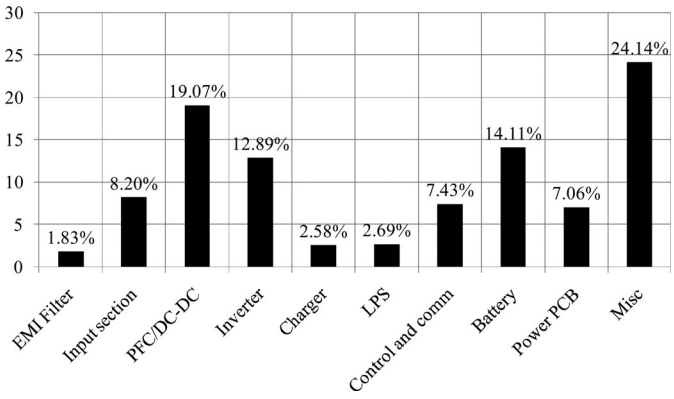

Fig. 23. Different subsystems and their costs of an online UPS.

B. Converter Efficiency Benefit

In order to test the efficiency benefit, the baseline UPS (25 kHz), and the GaN UPS (200 kHz) were tested under same operating conditions. Fig. 22 shows the comparative experimental efficiencies as obtained in online (mains input) and on-battery (battery input) modes. A resistive load was connected across the output. As seen from the results, the UPS with GaN offers much higher efficiency in online mode as compared to baseline, even though the converter was operated at eight times higher switching frequency. This was due to low switching and conduction losses of the GaN devices as against IGBTs. In on-battery mode, due to higher conduction losses in the buck–boost converter, the difference in efficiency is little less as compared to the online mode. However, the efficiency versus load trend line in both cases is similar.

The UPS with GaN devices offer better efficiency, and hence, low losses in both the operating modes as compared to the baseline. As a result, the GaN UPS needs smaller heat sinks than the baseline.

C. Cost Benefit

Fig. 23 shows different subsystems used in the baseline UPS and their percentage wise cost distribution. The subtotal cost attributed to the magnetics (inductors and transformers), output filter capacitor, switching devices, heatsink, and gate driver is around 26% of the total cost as shown in Table III. The switching frequency has direct or indirect impact on the above costs. Remaining 74% cost can be considered to be the fixed cost applicable to both baseline and GaN UPS units, where fixed costs are the costs associated with the modules containing no major power electronics converter such as bias power supply, control and communication cards, power printed circuit board (PCB) (without component), battery, fan, circuit breakers, relays and enclosure and their accessories. The cost breakup for the GaN UPS is also shown in Table III. As per the quotation received from the device manufacturer, the costs of the GaN switch and GaN diode used in this paper are very close to the costs of the equivalent Si devices used in the baseline UPS. As seen from the table, there is a net saving of around 6.8% by designing the UPS with GaN-based devices. Some additional saving is expected to come from the enclosure due to size reductions. On the other hand, if only power electronic converters are considered (excluding the fixed cost), there is a net saving of 25.7%.

TABLE III
COST SAVING OPPORTUNITIES IN ONLINE UPS

Items	Baseline UPS	GaN UPS
	% cost	% cost
Magnetics	10.75 %	5.57%
Filter Capacitor	4.52 %	2.26 %
Semiconductor	6.63%	6.63 %
Heat Sink	2.22%	1.78 %
Gate Drivers	2.22%	3.33%
Fixed cost	73.66 %	73.66 %

VII. ISSUES AND CONCERNS USING GAN

This section describes the lessons learnt so far and few critical issues and concerns while working with GaN based devices operating at higher switching frequency.

A. PCB Layout

GaN devices require a very tight layout [36], [37]. The paths for all high-frequency current commutating loops should be as small as possible. The gate driver outputs should be directly connected to the device gate and source terminals using shortest possible track. Decoupling capacitors should be placed in appropriate places in the circuit to provide a shortest path for the high frequency commutating current and control the voltage stresses across the devices.

B. Gate Driver

A fast gate driver chip with low output impedance, and low propagation delays is required to drive the GaN switch [37]. The traditional gate drivers may not be useful in this regard. Already different manufacturers have started releasing suitable fast gate drivers for driving the GaN switches. The newer gate drivers might cost more as compared to traditional ones.

C. Negative Gate Drive Voltage

In case of inverter application, a negative gate drive voltage is desirable to turn OFF the GaN switch due to its low threshold voltage ($\sim$1 V). It is observed that due to miller capacitance effect, there is lots of oscillation in the gate waveform when the complementary device is turned ON and OFF.

D. Stabilizing the Gate Waveform

The GaN switch has very low gate to source and gate to drain capacitances. Further, it has got extremely low switching times. As a result, high-frequency oscillations are observed in the gate–source voltage waveform around the switching instants, when the drain voltage changes at a faster rate. These oscillations caused unwanted device turn ON, followed by arm short circuit [38] in a half-bridge inverter. In this study, these oscillations were controlled by connecting an additional capacitor (1 nF) and damping resistor (1 kΩ) across the gate and source terminals of each GaN switch. Further, as explained in Section II-B, a series gate resistor helps stabilize the gate waveform.

E. Inverter Dead-Time Effect

A 250-ns dead time was used between the top and bottom devices of the half-bridge inverter to prevent an arm short-circuit failure [38] and have safer operation at 200-kHz switching frequency. It is around 10% of half the switching period. As the switching frequency is increased, the effect of dead time cannot be neglected. The inverter needs higher dc bus voltages to prevent over modulation, and hence, voltage clamping at the output voltage.

F. Paralleling

The paralleling of GaN switch and diode needs a very tight layout [36]. The distance between the gate driver and the gate terminals of all the GaN switches (connected in parallel) should be minimized as much as possible [37]. The gate drive return currents should preferably return to the driver through a plane.

VIII. Conclusion

In this paper, a 600 V normally OFF type GaN switch (cascode structure) and GaN diode were investigated in detail from different perspectives. The following conclusions can be drawn.

1) The experimental switching and conduction loss models of these devices matched well with the datasheet-based models. These can be used to design the thermal system of the converter.
2) Experimental results pertaining to different power converters showed that the GaN devices result in very low switching losses. As a result, GaN devices can be used in applications requiring high switching frequency and higher efficiency.
3) The performance of Si MOSFET (i.e., CoolMOS) in boost converter experiment was found to be very close to the performance of the GaN switch. This was, however, possible due to use of GaN diode as the boost diode. The Si MOSFET could not offer such performance with any Si fast recovery diode. Again, the Si MOSFET technology has almost reached its maturity level, whereas the GaN technology is just evolving. It has long journey toward its maturity. In this study, it is shown that a Revision-0 GaN switch and GaN diode samples can offer slightly better performances than CoolMOS. A matured GaN switch can be expected to offer superior performance in the near future compared to its current performance.
4) Like IGBT, the GaN switch did not have short-circuit capability (i.e., 400 V across it for 10 μs). However, it can tolerate worst case short circuit for 10 μs duration up to a dc bus voltage of 200 V.
5) Like MOSFET, the GaN switch and GaN diode can be paralleled to increase the power rating of the converter.
6) The performance of the GaN diode was superior to the performance of equivalent Si diode, and was very close to the performance of the equivalent SiC diode.
7) The use of GaN devices in online UPS system enabled us to increase the converter switching frequency from 25 kHz (baseline UPS) to 200 kHz. It resulted in more than 70% reduction in size, volume and PCB footprint of the associated magnetic components, and 40% reduction in the volume of the inverter output filter capacitor. Further, its higher efficiency with respect to baseline enabled us to reduce the size of the heatsink and associated cooling system by more than 20%. Overall, 20% size reduction was achieved in GaN UPS with respect to baseline UPS.
8) The use of GaN devices resulted in efficiency increase of more than 6% in online mode and more than 3% in on-battery mode. This will help us to meet stringent energy standards, and to increase the battery backup time in on-battery mode.
9) The cost analyses showed that the total cost of different power converters used in an online UPS system can be reduced by 25% by using GaN devices.
10) Finally, if the device manufacturers can meet their forecasted pricing target after launching their devices, the GaN devices will be widely used in majority applications to obtain SiC device performances at today's Si price.

References

[1] Energy star. (2010). [Online]. Available: http://www.energystar.gov/
[2] J. Millán, "A Review of WBG power semiconductor devices," in *Proc. IEEE Int. Semicond. Conf.*, Oct. 2012, pp. 57–66.
[3] K. Shenai, "Reliability of wide bandgap semiconductor power switching devices," in *Proc. IEEE Nat. Aerosp. Electron. Conf.*, Jul. 2010, pp. 322–327.
[4] N. Zhang, V. Mehrotra, S. Chandrasekaran, B. Moran, L. Shen, U. Mishral, E. Etzkorn, and D. Clarke, "Large area GaN HEMT power devices for power electronic applications: switching and temperature characteristics," in *Proc. IEEE 34th Power Electron. Spec. Conf.*, Jun. 2003, pp. 233–237.
[5] M. A. Khan, G. Simin, S. G. Pytel, A. Monti, E. Santi, and J. L. Hudgins, "New developments in gallium nitride and the impact on power electronics," in *Proc. IEEE 36th Power Electron. Spec. Conf.*, Jun. 2005, pp. 15–26.
[6] S. Tiwari, T. Undeland, S. Basu, and W. Robbins, "Silicon carbide power transistors, characterization for smart grid applications," in *Proc. 15th IEEE Int. Power Electron. Motion Control Conf.*, Novi Sad, Serbia, 2012, pp. 2-1–2-8.

[7] B. Hughes, J. Lazar, S. Hulsey, D. Zehnder, D. Matic, and K. Boutros, "GaN HFET switching characteristics at 350 V/20 A and synchronous boost converter performance at 1 MHz," in *Proc. IEEE 27th Appl. Power Electron. Conf.*, Feb. 2012, pp. 2506–2508.
[8] S. N. Mohammad, A. A. Salvador, and H. Morkoc, "Emerging gallium nitride based devices," *Proc. IEEE*, vol. 83, no. 10, pp. 1306–1355, Oct. 1995.
[9] M. Danilovic, Z. Chen, R. Wang, F. Luo, D. Boroyevich, and P. Mattavelli, "Evaluation of the switching characteristics of a gallium-nitride transistor," in *Proc. Energy Convers. Congr. Expo.*, Sep. 2011, pp. 2681–2688.
[10] J. Shealy, J. Smart, M. Poulton, R. Sadler, D. Grider, S. Gibb, B. Hosse, B. Sousa, D. Halchin, V. Steel, P. Garber, P. Wilkerson, B. Zaroff, J. Dick, T. Mercier, J. Bonaker, M. Hamilton, C. Greer, and M. Isenhour, "Gallium nitride (GaN) HEMT's: Progress and potential for commercial applications," in *Proc. 24th IEEE GaAs IC Symp.*, 2002, pp. 243–246.
[11] U. K. Mishra, "Gallium nitride electronics: Watt is the limit?" in *Proc. IEEE Device Res. Conf.*, Jun. 2004, vol. 1, pp. 3–5.
[12] M. N. Yoder, "Gallium nitride past, present, and future," in *Proc. IEEE High Speed Semicond. Devices Circuits*, Aug. 1997, pp. 3–12.
[13] A. Kistchinsky, "GaN solid-state microwave power amplifiers-State-of-the-art and future trends," in *Proc. IEEE Microw. Telecommun. Technol.*, Sep. 2009, pp. 11–16.
[14] J. S. Glaser, J. J. Nasadoski, P. A. Losee, A. S. Kashyap, K. S. Matocha, J. L. Garrett, and L. D. Stevanovic, "Direct comparison of silicon and silicon carbide power transistors in high-frequency hard-switched applications," in *Proc. IEEE 26th Appl. Power Electron. Conf.*, Mar. 2012, pp. 1049–1056.
[15] J. Biela, M. Schweizer, S. Waffler, and J. W. Kolar, "SiC versus Si-Evaluation of potentials for performance improvement of inverter and DC–DC converter systems by SiC power semiconductors," *IEEE Trans. Ind. Electron.*, vol. 58, no. 7, pp. 2872–2882, Jul. 2011.
[16] D. Aggeler, F. Canales, J. Biela, and J. W. Kolar, "Dv/Dt-control methods for the SiC JFET/Si MOSFET cascode," *IEEE Trans. Power Electron.*, vol. 28, no. 8, pp. 4074–4082, Aug. 2013.
[17] G. Xun, I. Josifović, and J. A. Ferreira, "Modeling and reduction of conducted EMI of inverters with SiC JFETs on insulated metal substrate," *IEEE Trans. Power Electron.*, vol. 28, no. 7, pp. 3138–3146, Jul. 2013.
[18] IMS Research report. (2010). SiC & GaN power semiconductors. [Online]. Available: http://www.imsresearch.com/news-events/press-template.php?pr_id=2704
[19] A. Lidow, "Is it the end of the road for silicon in power conversion?," in *Proc. IEEE 6th Int. Conf. Integr. Power Electron. Syst.*, Mar. 2010, pp. 1–8.
[20] A. Hensel, C. Wilhelm, and D. Kranzer, "Application of a new 600 V GaN transistor in power electronics for PV systems," in *Proc. 15th IEEE Int. Power Electron. Motion Control Conf.*, Novi Sad, Serbia, 2012, pp. 1–5.
[21] J. -Kim and C. Kim, "A DC-DC boost converter with variation-tolerant MPPT technique and efficient ZCS circuit for thermoelectric energy harvesting applications," *IEEE Trans. Power Electron.*, vol. 28, no. 8, pp. 3827–3833, Aug. 2013.
[22] Yu Gu and D. Zhang, "Interleaved boost converter with ripple cancellation network," *IEEE Trans. Power. Electron.*, vol. 28, no. 8, pp. 3860–3869, Aug. 2013.
[23] A. Urtasun, P. Sanchis, and L. Marroyo, "Adaptive voltage control of the DC/DC boost stage in PV converters with small input capacitor," *IEEE Trans. Power. Electron.*, vol. 28, no. 11, pp. 5038–5048, Nov. 2013.
[24] D.-H. Kim, G.-Y. Choe, and B.-K. Lee, "DCM analysis and inductance design method of interleaved boost converters," *IEEE Trans. Power. Electron.*, vol. 28, no. 10, pp. 4700–4711, Oct. 2013.
[25] C.-L Wei, C.-H Chen, K.-C. Wu, and I.-T. Ko, "Design of an average-current mode noninverting buck-boost converter with reduced switching and conduction losses," *IEEE Trans. Power Electron.*, vol. 27, no. 12, pp. 4934–4943, Dec. 2012.
[26] J. M. Alonso, D. Gacio, F. Sichirollo, A. R. Seidel, and M. A. Dalla Costa, "A straightforward methodology to modeling high power factor AC-DC converters," *IEEE Trans. Power Electron.*, vol. 28, no. 10, pp. 4723–4731, Oct. 2013.
[27] A. Kulkarni and V. John, "Mitigation of lower order harmonics in a grid-connected single-phase PV inverter," *IEEE Trans. Power Electron.*, vol. 28, no. 11, pp. 5024–5037, Nov. 2013.
[28] F. Ma, A. Luo, X. Xu, H. Xiao, C. Wu, and W. Wang, "A Simplified power conditioner based on half-bridge converter for high-speed railway system," *IEEE Trans. Ind. Electron.*, vol. 60, no. 2, pp. 728–738, Feb. 2013.
[29] A. Lahyani, P. Venet, A. Guermazi, and A. Troudi, "Battery/Supercapacitors combination in uninterruptible power supply (UPS)," *IEEE Trans. Power. Electron.*, vol. 28, no. 4, pp. 1509–1522, Apr. 2013.
[30] B. Tamyurek, "A High-Performance SPWM controller for three-phase UPS systems operating under highly nonlinear loads," *IEEE Trans. Power. Electron.*, vol. 28, no. 8, pp. 3689–3701, Aug. 2013.
[31] B. M. Green, "Cascode connected AlGaN/GaN HEMT on SiC substrates," *Proc. IEEE Microw. Guided Wave Lett.*, pp. 316–318, Aug. 2000.
[32] N. Mohan, T. M. Undeland, and W. P. Robbins, *Power Electronics*. Hoboken, NJ, USA: Wiley, 2003.
[33] I. Cohen, T. Gang Zhu, L. Liu, M. Murphy, M. Pophristic, M. Pabisz, M. Gottfiied, B. S. Shelton, B. Peres, A. Ceruzzi, and R. A. Stall, "Novel 600 V GaN Schottky diode delivering SiC performance at Si prices," in *Proc. IEEE 20th Appl. Power Electron. Conf.*, Mar. 2005, vol. 1, pp. 311–314.
[34] O. Al-Naseem, R. W. Erickson, and P. Carlin, "Prediction of switching loss variations by averaged switch modeling," in *Proc. IEEE 15th Appl. Power Electron. Conf.*, Feb. 2000, vol. 1, pp. 242–248.
[35] A. Bhalla, S. Shekhawat, J. Gladish, J. Yedinak, and G. Dolny, "IGBT behavior during desat detection and short circuit fault protection," in *Proc. IEEE 10th Int. Symp. Power Semicond. Devices ICs*, Jun. 1998, pp. 245–248.
[36] J. Strydom and M. De Rooji, "Paralleling eGaN® FETs—Part 2," *Power Electron. Mag.*, vol. 36, no. 9, Sep. 27, 2011.
[37] X. Youhao, M. Chen, K. Nielson, and R. Bell, "Optimization of the drive circuit for enhancement mode power GaN FETs in DC-DC converters," in *Proc. IEEE 27th Appl. Power Electron. Conf.*, Feb. 2012, pp. 2467–2471.
[38] Z. Xu and F. Wang, "Experimental investigation of Si IGBT short circuit capability at 200 °C," in *Proc. IEEE 27th Appl. Power Electron. Conf.*, Feb. 2012, pp. 162–168.

Radoslava Mitova received the M.S degree in electric engineering from the Technical University of Sofia, Sofia, Bulgaria, in 2001, and the Ph.D. degree in power electronics from the National Polytechnic Institute of Grenoble, France, in 2005.

She worked for PRIMES Lab (Tarbes) on high voltage architectures with medium voltage transformer for railway traction. She joined Schneider Electric, in 2007, as power electronic engineer. She is currently working on new material power semiconductors as SiC and GaN in industrial application inverters.

Rajesh Ghosh received the Ph.D. degree in electrical engineering from the Indian Institute of Science Bangalore, India, in 2007.

He is a staff Electrical Engineer at Schneider Electric, Bangalore, India. His research interests include modeling, analysis, design, and control of power electronic converters. Prior to joining Schneider Electric, he has worked at GE GRC Bangalore, and CESC Ltd., Kolkata, India

Uday Mhaskar received the Ph.D. degree from the Indian Institute of Technology Bombay, Powai, India, in 2003.

His research areas include control system design, power electronics and drives, renewable energy and energy storage technologies. He is a Staff Engineer at Schneider Electric, Bangalore, India.

Damir Klikic received the Master's degree in electrical engineering from the University of Zagreb, Croatia, in 1985.

He has been with American Power Conversion from 1991 and with Schneider Electric from 2007 where he has been involved with power converters, UPS systems, control, and modeling. In his current role hes leading applied research and study of emerging technologies, applications, and markets. He is the author and coauthor of more than 10 patents and scientific papers.

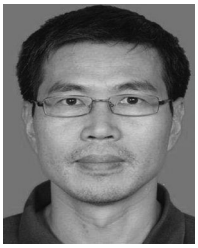

Miao-xin Wang received the Engineer degree in automatics and power electronics from ENSEEIHT, Toulouse, France, in 1989, and the Ph.D. degree in electrical engineering from INPT, Toulouse, in 1992.

He joint Schneider Electric in 1993, before moving to UPS development and RD management within MGE UPS System from 2000 to 2007 and Eaton Electrical from 2007 to 2011. Since 2011, he has been leading Advanced Electronics and Power Electronics team, within Schneider Electric Corporate Technology Innovation Department, Grenoble, France. He is the author and coauthor of several papers and patents on harmonic filtering, low-harmonic converter topology, and UPS topology.

Alain Dentella is with Schneider group since 1984. He was Electronic Designer from 1984 to 2010 in protections relays for medium voltage. Since, 2010, he has been with technical research in Power Electronics & Advanced Electronics.